Proceedings World Geothermal Congress 2020+1
Reykjavik, Iceland, April - October 2021

High Resolution Gravity Data to Characterize Density Variations and Reduce Uncertainty in Geothermal Reservoirs in the Geneva Basin (GB)

Guglielmetti L.*, Perozzi, L. *., Dupuy D.***, Martin F., ** Métraux V.***, Meyer, M.**, Mijic G.*, Moscariello A.*, Nawratil De Bono C.**Radogna P.V.**

*Department of Earth Sciences, University of Geneva. Rue des maraichers 13, 1205 Geneve (Switzerland)

**Services Industriels de Genève. Chemin du Château-Bloch 2, 1219 Le Lignon (Switzerland)

***GEO2X SA. Rue de Chamblon 34, 1400 Yverdon-les-Bains (Switzerland)

luca.guglielmetti@unige.ch

Keywords: gravity, high-resolution, uncertainty, inversion, geothermal reservoir, Geneva, GEothermie2020, sedimentary basin, GECOS

ABSTRACT

This paper focuses on the acquisition and processing of gravity data collected in the Canton of Geneva in the framework of the InnoSuisse funded project GECOS (Geothermal Energy Chance of Success). The goals of GECOS is to reduce the costs and the exploration risk for geothermal exploration by integrating high resolution data acquisitions such as gravity, S-waves reflection seismic and 3D DAS VSP (Distributed Acoustic Sensing Vertical Seismic Profiling). The main geological challenges in geothermal exploration in the Geneva area are the characterization of the lithological heterogeneities and the fault zones affecting potential geothermal targets in the Quaternary sediments, Oligecene Molasse sequence and the Mesozoic Units. The study area covers the central part of the Canton of Geneva and overlaps with the location of two geothermal exploration wells drilled by SIG in the framework of the Geothermie 2020 program. A total of 1714 new stations were collected in 71 days of field work thanks to the collaboration between the University of Geneva and GEO2X SA. The goal of the survey has been to constrain the lateral density variations associated to lithological anisotropies in the Quaternary, Oligecene Molasse and in the Mesozoic carbonate sequence. The results of the survey showed that the new stations produced a dramatic increase in resolution compared to the gravity data available at the regional scale. In particular Quaternary deposits are much better constrained than before, which is a crucial step forward as these sediments are known to be lithologically and geometrically heterogeneous and locally can host hydrocarbon gas pockets, which can represent an element of risk for drilling operations. 3D inversion processing allowed producing a realistic 3D density model down to about 1000m in depth, where the main present-day geothermal targets are located, proving that gravity can be a powerful tool for prospection and possibly for time-lapse monitoring of production.

1. INTRODUCTION

The increased energy demand together with the political vision of reducing the use of fossil fuels for heat production in the Canton of Geneva triggered the development of medium to long term activities, under the umbrella of the Geothermie 2020 program (Moscariello, 2016). This program aims at exploring and ultimately implementing geothermal energy focusing first on heat production and storage, and then on power production. The program is driven by the Services Industriels de Genève (SIG), the Geological Survey of the Canton of Geneva (GESDEC) and is supported by national authorities such as the Swiss Federal Office of Energy (SFOE) and national research programs (i.e. the Swiss Competence Centre for Energy Resources, (SCEER). The exploration activities carried out since now allowed identifying potential geological targets at shallow/medium (500-3000 m) to large depth (>3000 m) depths. to combine heat and power production.

The identification and characterization of the subsurface prior drilling is crucial to define potential geothermal targets. 2D seismic has proved to be the most effective method to image the Mesozoic formations in the Geneva Basin (GB) (Clerc et al., 2015; Moscariello, 2016; Moscariello et al., 2020), but showed some limits in delineating shallow Quaternary deposits, and was not designed to illuminate deep structures (>4000 m) and thus cannot provide accurate spatial information about the deep sedimentary units deep Permo-Carboniferous grabens.

In the framework of a continued desire to improve the understanding of the subsurface in the GB, GECOS (Geothermal Exploration Chance Of Success) aims at collecting new geophysical data (gravity, S-waves active seismic and 3D Distributed Acoustic Sensing Vertical Seismic Profiling 3D DAS VSP) to improve the subsurface imaging at the local scale, reduce the subsurface uncertainty and assess the add value of information provided by such acquisitions compared to existing fata. Specifically, in this paper we use existing and newly acquired gravity data to evaluate the potential of application of gravity method which, despite being a well-established geophysical investigation technique, this was never been considered as a tool to support geothermal exploration in the Geneva area.

In this paper, we aim at:

- Processing the gravity data using a pseudo-tomography approach to delineate gravity anomalies associated with the main geological features
- Quantifying the uncertainty associated to gravity data
- Run 3D inversion to produce a 3D density model over a selected study area

2. GEOLOGIC SETTING

The Geneva Basin (GB) covers an area of about 2000 km^2 extending from the town of Nyon to the NE, down to Vuache Mountain to the SW and it is limited by the Jura Haute-Chaine to the NW and by the subalpine nappes towards SE.

The GB is the westernmost part of the North Alpine Foreland Basin that extend from the Savoy region in France to Linz in Austria (Kuhlemann & Kempf, 2002). Four major lithological units are recorded at depth (Kempf & Pfiffner, 2004; Kuhlemann & Kempf, 2002; Mazurek, Hurford, & Leu, 2006) the crystalline basement including the Permo-Carboniferous troughs (Moscariello et al., 2014), its sedimentary cover composed respectively of Mesozoic carbonatic units and Cenozoic sediments (Figure 1).

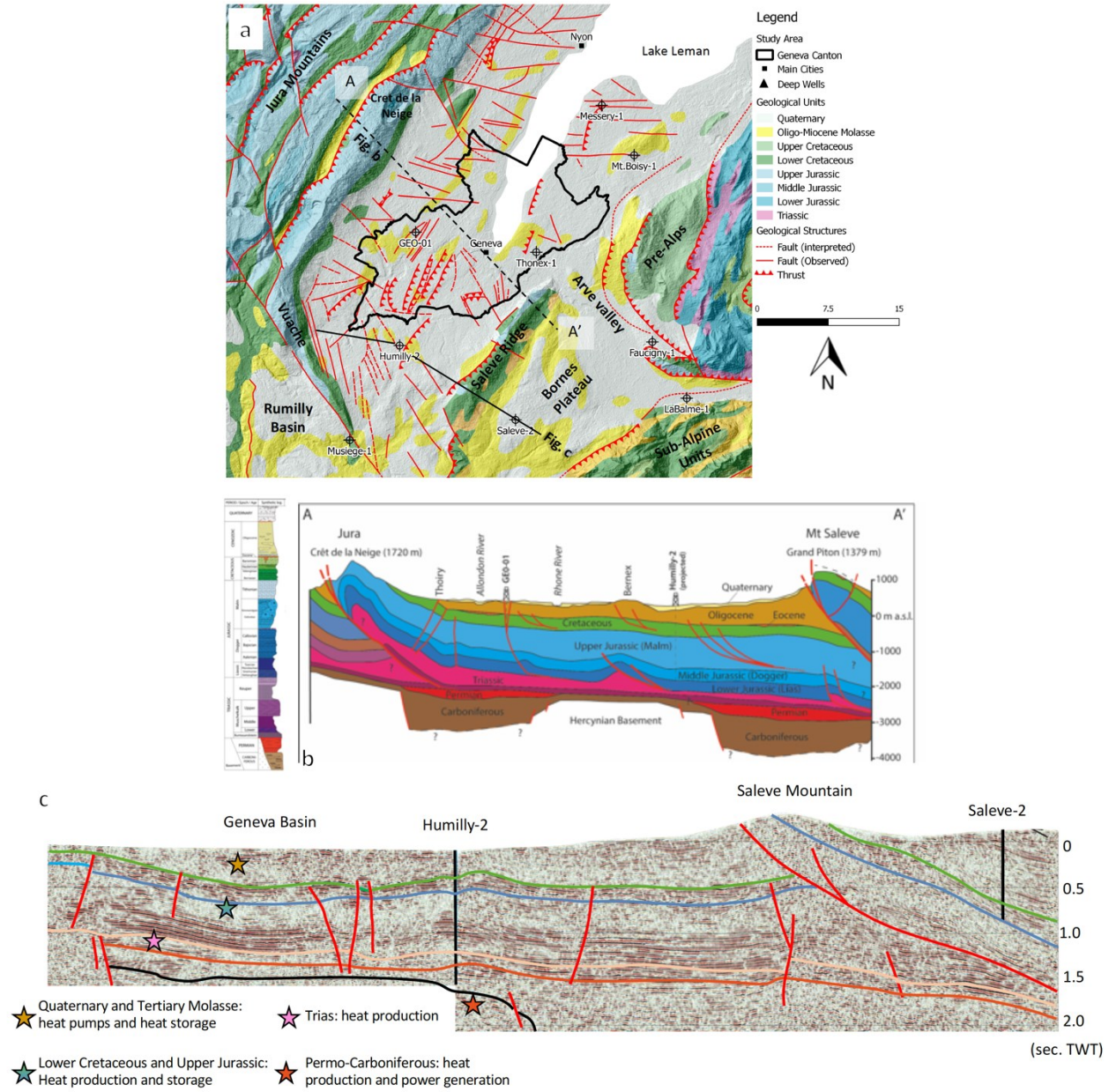

Figure 1 - a) Geological map over the Geneva Basin with indication of the main deep wells (modified. from Brentini, 2018); B) Cross section cutting though the GB (modified from Moscariello et al., 2020). C. Seismic section showing the general structural setting and the main geothermal targets (modified from Moscariello, 2016)

From bottom to top, the stratigraphic unites in the GB are resumed in Table 1:

Table 1 - Schematic stratigraphy if the geologic units in the Geneva Basin

Era	Period	Epoch	Lithology
Cenozoic	Quaternary		Heterogeneous, locally thick, glacial and fluvio-glacial and glacio-lacustrine sequences mostly genetically related to the last Würmian glaciation.
	Paleogene	Oligocene	In the GB area only the Lower Freshwater Molasse is observed in outcrops and borehole records and can reach a thickness of 1300m in the southern part of the region, where the Thônex-01 well is located (Guglielmetti et al. 2020).
Mesozoic	Cretaceous	Lower	Fine grained/bioclastic and fine quartz-rich bioturbated limestones alternating with organic-rich marls accumulated with a shallow and warm water environment. The top of the Lower Cretaceous is characterized by an erosive and highly karstified sequence boundary surface.
	Jurassic	Malm	Competent, often massive, shallow-marine platform carbonate deposits. locally the whole Malm interval could be highly fractured and karstified. Biothermal reefs facies are developed mainly during the Kimmeridgian-Thitonian interval and make this horizon a potentially interesting geothermal target where hot waters can circulate. The Purbeckian formation represents the last Jurassic stage and is more argillaceous than the underlying units.
		Dogger	Intercalations of marls and crinoidal limestone with quartz-detritic intervals toward the upper part.
		Lias	Bioclastic muddy limestones in the lower part and the organic-rich Posidonia shales as upper unit.
	Trias	Late	Succession of clastic, carbonates and evaporites overall reaching up to 500 m in thickness. The Triassic succession is typically capped by a shale unit known as the Rhaetian.
Paleozoic	Permian		Crystalline basement which only crops out in the Alps, southwards the GB. The basement is often affected by SW-NE oriented depressions (Moscariello et al., 2014; Moscariello, 2019) filled with several thousands of meters of Permo-Carboniferous sediments.
	Carboniferous		

The tectonic evolution of the GB is associated with the alpine compressional phase that caused the decoupling of the sedimentary succession from the basement by a detachment surface occurring on the Triassic evaporites (Affolter & Gratier, 2004; Arn et al., 2005; Guellec, et al., 1990; Sommaruga, 1999). Additionally, inherited basement reliefs and normal faults bounding Permo-Carboniferous troughs might have played a role in the nucleation of the Mesozoic north-westward thrusts observed in the SE sector of the Geneva Basin and Bornes Plateau (Gorin, et al., 1993; Signer & Gorin, 1995).

In response to the alpine compression, the Mesozoic and Cenozoic sedimentary cover of the GB underwent some shortening locally coupled to a rotational motion. This shortening was absorbed through the structuration of the fold and thrust reliefs of the Jura arc mountains during the late Miocene and Early Pliocene (Affolter & Gratier, 2004; Homberg, et al., 2002; Meyer, 2000) and by the coeval formation of accommodation of strike-slip faults. The most relevant surface evidence of such structures is the NW-SE Vuache fault (Charollais et al., 2013), which crosscuts the entire basin and bounds the western side of the study area.

In the GB, apart from the regional Vuache fault, series of smaller-scale NW-SE striking left-lateral wrench faults affect the southwestern part of the Geneva area. Unlike the Vuache fault, no obvious connections between these structures and the Jura Mountain can be drawn across the study area (Brentini, 2018; Rusillon, 2018) as suggested in previous interpretations (Signer & Gorin, 1995). Towards the northeast of the basin, the structural configuration is dominated by E-W striking faults. NW-SE and E-W strike slip faults occur as series of sub-vertical individual faults often affecting most of the Mesozoic sequence, down to the Triassic decollement surface, with associated smaller-scale sets of conjugates. Upward extension through the Cenozoic interval of the most important faults often appears as flower structures. This shallow subsurface expression is consistent with fault geometries observed in Oligecene Molasse outcrops (Angelillo, 1983; Charollais et al., 2007). The maximum horizontal stress orientation in the study area shows two main trends: central and eastern part have a WNW-ESE to NW-SE S_H orientation, whereas the south-western region is controlled by a NE-SW orientation (Becker, 2000).

3. GRAVITY DATA IN THE STUDY AREA

Gravity method is a standard geophysical subsurface exploration technique, which applications in different geological settings are largely documented in literature (Allis, et al. 2000; Blakely, 1995; Guglielmetti, et al., 2013; Reynolds, 1996; Telford, et al. 1990; Uwiduhaye et al. 2018; Wilkinson et al. 2017). The main source of data for the study area is the gravimetric Atlas of Switzerland (Olivier et al. 2002) with an average station density of 0.3 station/km^2. In addition, more data for the surrounding French areas are available from the International Gravimetric Bureau BGI at a less dense station distribution (average 15 station/100km^2). A total of 1714 new gravity stations have been collected in the framework of the GECOS project (Figure 2).

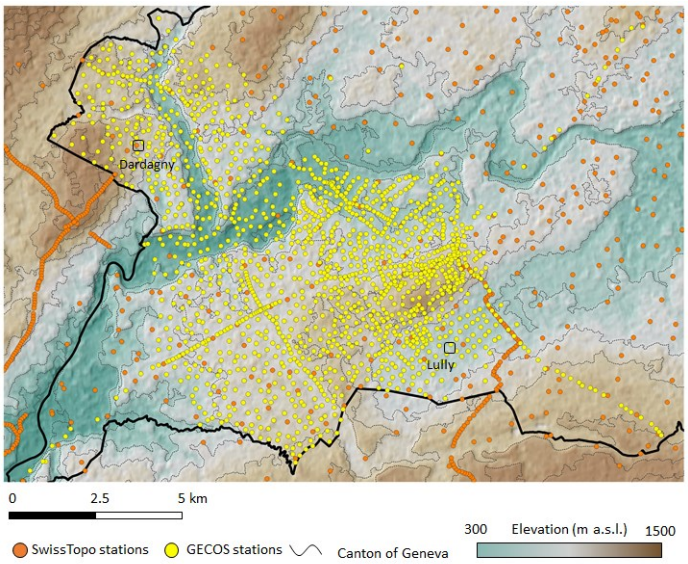

Figure 2 – Location of the survey area and the Gravimetric Atlas of Switzerland stations and the stations collected in the framework of the GECOS project

On a regional scale across the whole Molasse Plateau, Kahle, et al., 1976 and Klingele, 2006 showed a clear gravity regional NW-SE oriented trend of the Molasse basin, controlled by the deepening of the crust towards the Alpine front.

Gravity data were collected in the Geneva area and surrounding regions for hydrocarbon-resources exploration, and research studies. Gravity survey carried out across the whole Geneva canton covering the area with 3 stations per km^2 (Poldini, et al., 1963), showed the sequence of NE-SW oriented negative and positive anomalies, crossing the study area. The formers are associated with glacial valleys filled with quaternary deposits. The latter were interpreted as morphological features of the transgressive contact of the Oligocene Molasse on the Mesozoic units. Vertical gravity gradient was used to infer density variations in the quaternary filling (Montadon, 2000) across a limited area in the north-eastern part of the Geneva Canton while lateral and vertical heterogeneities of Quaternary to Cretaceous sedimentary layers were refined combining gravity and inverted velocities from well data to density lateral variations models (Carrier, et al., 2017).

3.1. SURVEY DESIGN

The design phase involved:

1. the definition of the most appropriate distance between the new gravity station
2. the method to collect the coordinates XYZ for each station

Point 1 was defined according 3D gravity forward modelling using the GEOMOL 3D geological model (www.geomol.eu) as main geometrical constrain. The 3D model was populated with density values from literature data that are summarized in **Error! Reference source not found.** :

Table 2 – Density values available from literature data

Lithology	Density (kg/m^3)	Data Source	min	Max	AVG	SD	Q1	Median	Q3
Quaternary	2.33	Litterature*	1.80	2.54	2.25	0.33	2.10	2.33	2.47
Oligocene Molasse	2.50	Litterature*	2.00	2.64	2.42	0.21	2.25	2.50	2.56
Cretaceous	2.68	Litterature*	2.50	2.69	2.64	0.08	2.64	2.68	2.68
Malm	2.68	Thonex Well log	2.57	2.69	2.67	0.03	2.68	2.68	2.68
Dogger	2.68	Litterature*	2.61	2.68	2.67	0.03	2.68	2.68	2.68
Lias	2.68	Litterature*	2.12	2.68	2.57	0.25	2.68	2.68	2.68
Trias	2.62	Humilly Well log	2.44	2.83	2.65	0.10	2.63	2.68	2.68
P.C. through	2.55	Humilly Well log	2.35	2.62	2.54	0.05	2.55	2.57	2.57
Crystalline Basement	2.67	Litterature*	2.60	2.83	2.69	0.07	2.67	2.67	2.71

*(Abdelfettah, et al., 2014; Altwegg, 2015; Mauri et al., 2017; Rusillon, 2018; Wagner, et al., 1999)

The gravity effect of the model was computed using GeoSoft Oasis Montaj software (3D GM-SYS toolset), which allows computing the 3D gravity effect of the known geological structures. The horizontal extent of the model has been defined to cover

the whole survey area and the vertical extent embeds the geologic units down to the crystalline basement to also take into account potential deep sources of gravity anomalies. The 3D geological model and the 3D density model are shown in Figure 3.

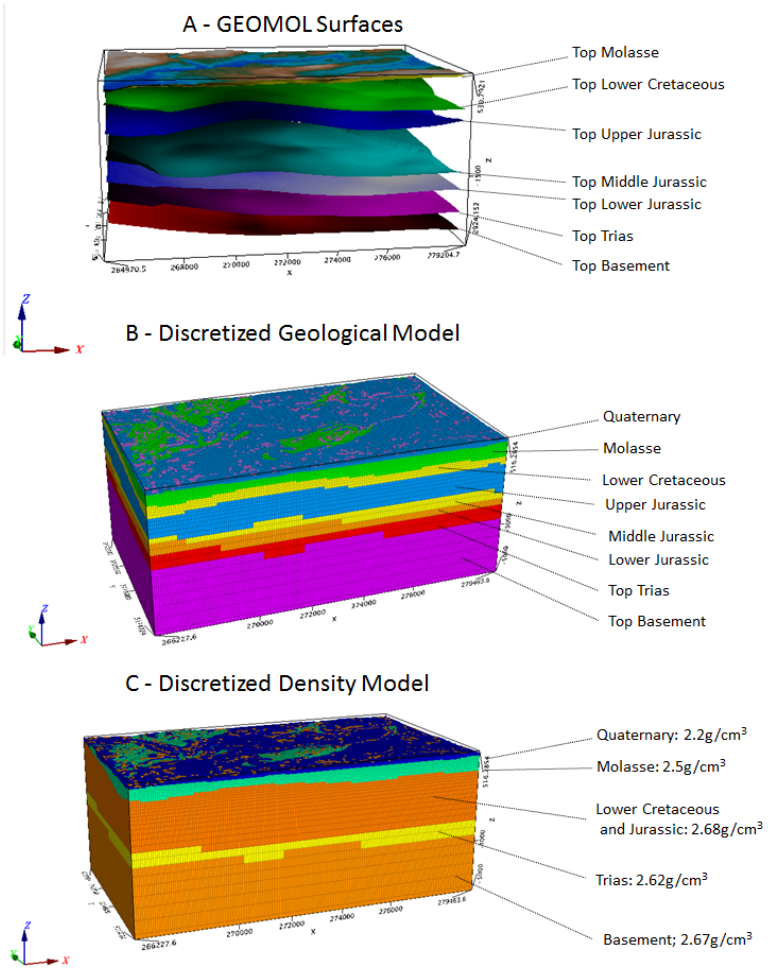

Figure 3 - 3D geological model and the 3D density model

3.2. DATA ACQUISITION

The survey was carried in 71 days adopting an approach aimed at optimizing at most the quality and the time of the acquisition. This was achieved by running cycles between control stations and by using the Geneva Canton cadastral points as reference for the coordinates XY of each station and the DPGS or the Geneva Canton LiDAR DTM for the Z coordinate.

Each phase started with a first day of testing and calibration recordings between the reference stations with the following order: 100000-20000-20002-20004-20006-20008-20010-20012-20000-100000 (Figure 4). This allowed us to connect our new stations to the absolute stations 100000 which allowed us to make a unique dataset with the Gravimetric Atlas of Switzerland. The 1st order base station 100000 was measured at the opening and the closure of each survey period.

All the other days the acquisition started at 2nd order base station 20000, at the opening and closure of each production day. Each day a 3rd order base stations 2000n was selected, depending on which portion of the survey area was covered each day to reduce transfers by car. This station was at the opening and closure of each daily loop. Every day two daily loops were measured. Some exceptions were made in cases the weather was too bad or the transfer time from and to the 3rd order station was too long, affecting the daily production. In those circumstances, only one loop at the 2000n station was done per day. At least five measurements were taken at each station. If a difference higher than 0.005mGal between following recordings was observed, additional records were collected until stable values were recorded.

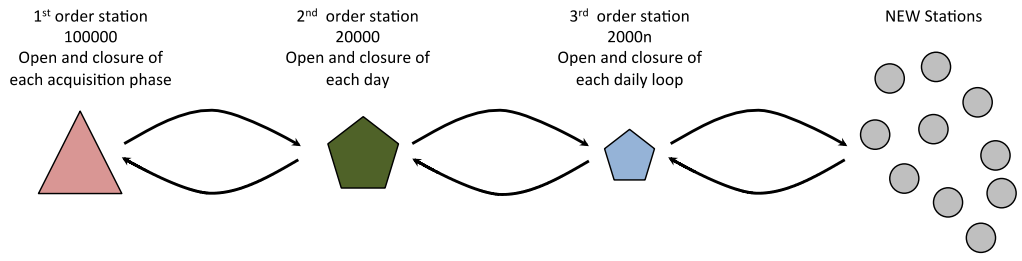

Figure 4 – Acquisition method

Figure 5 shows the Net daily production rate of new stations.

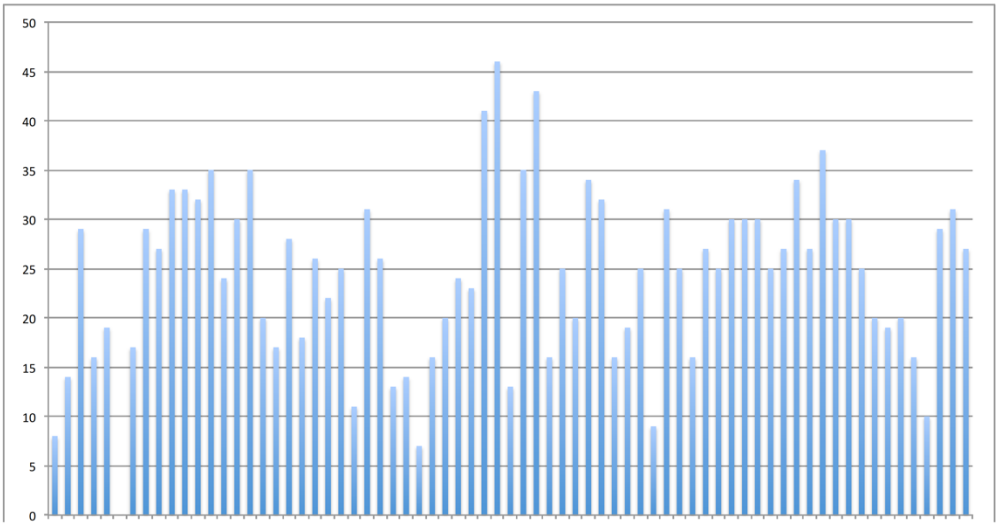

Figure 5 - Net daily production rate

3.2.1. QUALITY CONTROL

Daily QC was carried out at the end of the day in order to identify the records affected by measurement error. A total of 1719 new gravity stations were collected, and gravity was read at the Base 20002 at the opening and closure of each production day. Quality of the data was evaluated by checking the consistency of the daily drift plus random stations were also selected for measurements repeated along the whole survey. The maximum acceptable instrument drift at the 2nd order baste station 20000, was 0.1 mGal. If the drift exceeded this value, loops were repeated. Chart in Figure 6 shows the difference at the daily closure. All base closures were within 0.1 mGal.

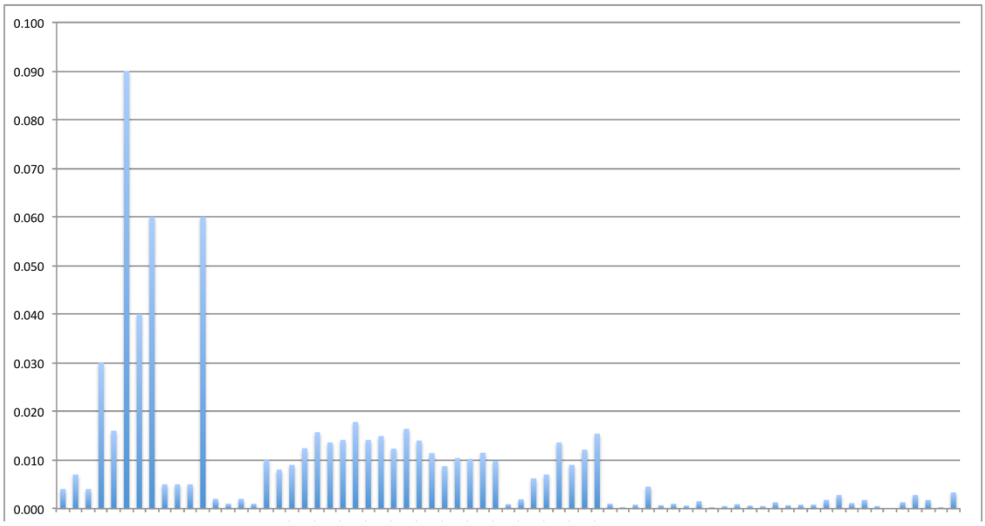

Figure 6 – Daily loop closure (mGal)

4. UNCERTAINTY QUANTIFICATION

One objective of the new acquisition campaign is to improve the knowledge of the subsurface density and better quantify its uncertainty. Starting from a gravity survey, we are able to produce a map of the complete Bouguer anomaly (CBA), as shown in figure 8. This map is a result of an interpolation of the observed anomaly at each survey location. However, since the distribution of the acquisitions stations could be more or less dense, we need to quantify the uncertainty related to the resulting interpolated map. Moreover, traditional interpolation methods such as Minimum Curvature or Inverse distance weighted gridding (IDW), do not consider the geological spatiality of the surveyed region. Over the last 20 years, stochastic simulation techniques have become popular as a way of generating realization that better represents the spatial variability in the subsurface (Doyen, 2007).

For this purpose, we propose a stochastic approach to produce several realizations of the CBA over the studied area, before and after the new gravimetric acquisition. First order statistics are then applied to estimate the variance at each pixel of the interpolated grid to evaluate uncertainty of the resulting interpolated map. We decided to use a Sequential Gaussian Simulation approach (Deutsch and Journel, 1992), a popular algorithm widely used in the oil and gas industry, to assess subsurface uncertainty. Firstly, we defined a random path the algorithm uses to visit each pixel of the simulation grid. Then, for each pixel, the algorithm computes a kriging distribution with hard data (gravimetric station data) and previously simulated data. From this distribution, the algorithms

draw randomly a value that is assigned to the pixel. Next, the algorithm move to the next pixel and the same process is repeated. By changing the seed of the path, we obtain randomly realization that have the same probability. Finally, we compute the variance of the ensemble of the realization (in our case 10) to estimate the uncertainty of the CBA.

The results are presented with the Figure 7, where the left figure shows the variance of 10 SGS realization using Swiss Atlas data only and in the right part the resulting variance of 10 realizations by adding the new, high resolution, data. The results show that by adding these new data, the uncertainty decrease considerably.

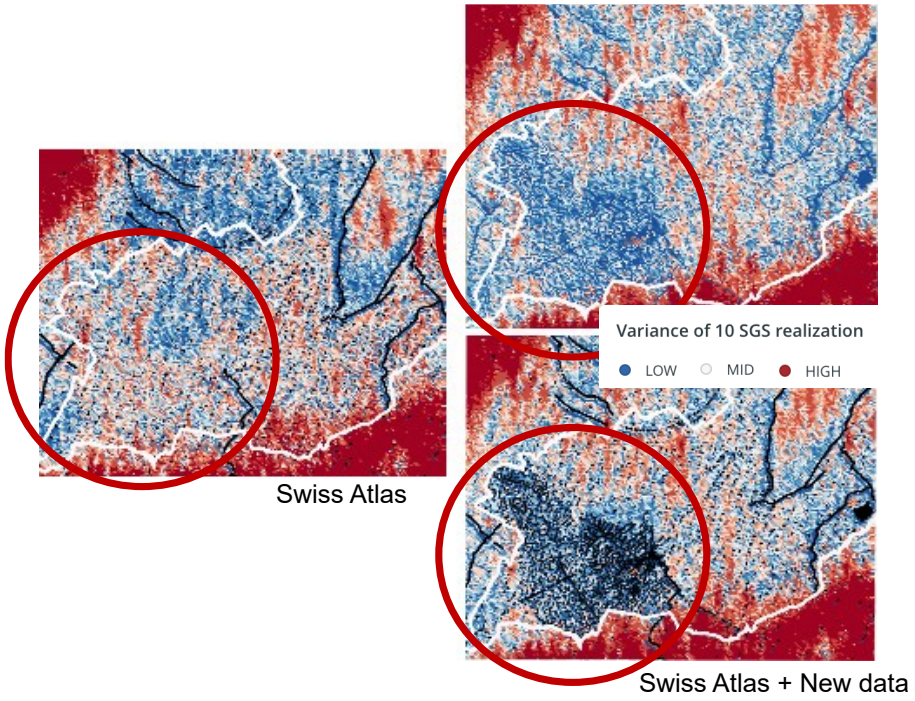

Figure 7 – Uncertainty evaluation with Swiss Atlas data (left) and Swiss Atlas + new campaign data in the right, by using an SGS approach.

4.1. GRAVITY DATA PROCESSING

Scintrex CG-5 gravity data are recorder digitally and were dumped to PC daily. Recorded data included:

- Line ID
- Station ID
- Gravity reading
- Standard Deviation
- X, Y Tilts
- Inner temperature deviation
- Internally calculated Earth tide correction
- Recording duration
- Number of rejected readings
- Time
- Date

CG-5 gravity meter calculates Earth Tide correction at each reading, based on the date and time of the reading at a user-defined location.

Data dumped from the gravity meter as .txt were imported in an Excel spread sheet to clean the records from outliers based on field notes and X-Y tilts or standard deviation. For each station the average of the gravity instrumental reading and time was calculated to get a unique Observed gravity ***Gobs*** value. Additionally, data were adjusted considering the height difference to the top of peg from the base gravimeter (0.003086mGal every centimetre) using the following equation:

Gobs (corr) = Gobs+ (h*0.003086)

Where:

- **Gobs (corr)** is the observed gravity corrected
- **Gobs** is the Observed Gravity
- **h** is the height difference to the top of peg from the base gravimeter
- **0.003086** is the gravity vertical gradient (mGal/cm)

The standard corrections were then applied to produce a Bouguer Anomaly map according to the following equations:

- **Drift** = $\frac{R_2-R_1}{T_2-T_1}$

Where **R1** and **R2** are the record at two stations and **T1** and **T2** are the time at which the measures were recorded

- **Latitude LC**= $978013.5 \cdot (1 + 0.005278895 \cdot sin^2 \varphi + 0.000023462 \cdot sin^4 \varphi)$

Where $\boldsymbol{\varphi}$ is the latitude expressed in Decimal degrees

- **Free Air FAC** = $0.3086 \cdot h$

Where **h** is the elevation of each station

- **Bouguer Plateau BPC** = $0.4191 \cdot \rho \cdot h$

Where **h** is the elevation of each station and $\boldsymbol{\rho}$ is the reference density, here used as 2.67 g/cm^3

- **Bouguer Anomaly BA** = Gobs-LC+FAC-BPC

The processing and analysis of the existing gravity data across the study area aimed at understanding the potential geological sources of the gravity signature in the study area, namely the Quaternary deposits, the Oligecene sediments and, the Upper Mesozoic carbonate sequence. The processing has been carried out using the software Geosoft Oasis Montaj version 9.4 (2018).

The processing followed the sequence shown in Figure 8.

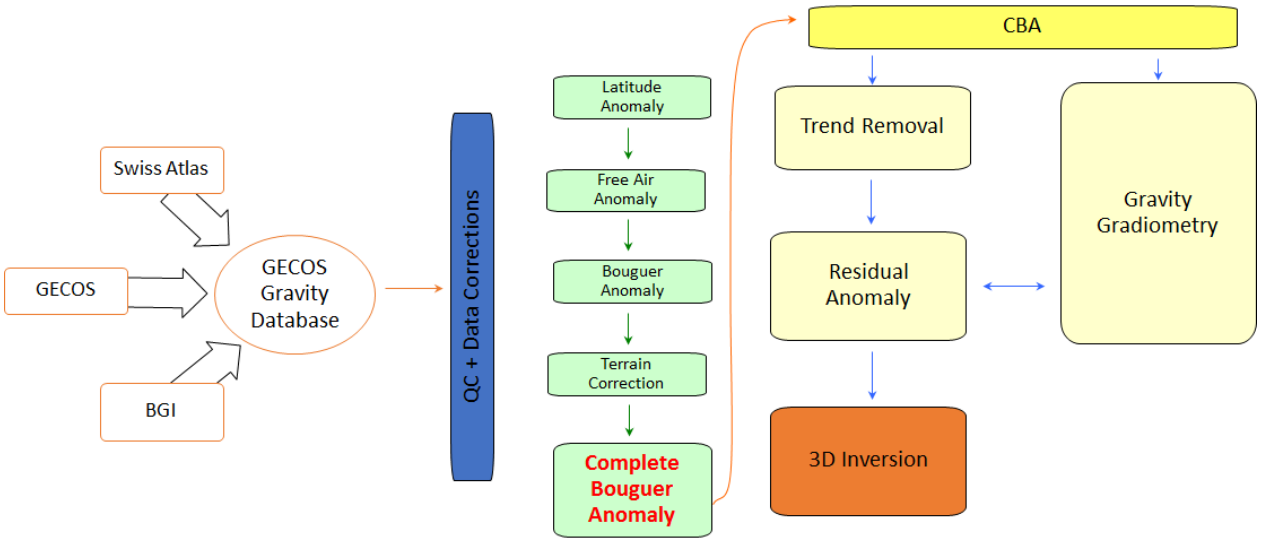

Figure 8 – Gravity processing workflow applied in this study

The processing consisted in the following steps:

- Combination of the data from the Gravimetric Atlas of Switzerland and the Bureau International de Gravimetrie (BGI), and quality control.
- Calculation of the Latitude, Free Air, and Bouguer anomalies as well as the Terrain correction to produce a Complete Bouguer Anomaly (CBA). The CBA was calculated using a reference density of 2.67 g/cm^3, which was constrained by using the Parasnis (1951) and Nettleton (1939) methods. Additionally, the Terrain correction was applied to the Bouguer Anomaly to account for thee gravity effect of masses above and under the measurement station and which were not taken into account by the plateau correction. The effect of topography is considered to be the classical distance of 167 km which is equal to an arc of 1.5° on the Earth. As the gravity effect decreases with the square of the distance, we used two different DEMs of different resolutions to calculate this effect. From the station to the distance of 1000 m, a high-resolution DEM with a grid size of 0.5m and a vertical accuracy of ±0.15 m. From 1000 m to 167 km, the ASTER Global Digital Elevation Model V002 with a grid size of about 30m and a vertical accuracy <15 m was used.
- Removal of the regional trend to produce a residual gravity anomaly representative of the gravity signature of the geological features of interest. The Complete Bouguer Anomaly shows a linear trend NW-SE oriented, which was removed to produce the Residual bouguer anomaly. The results of the processing are shown in Figure 9.

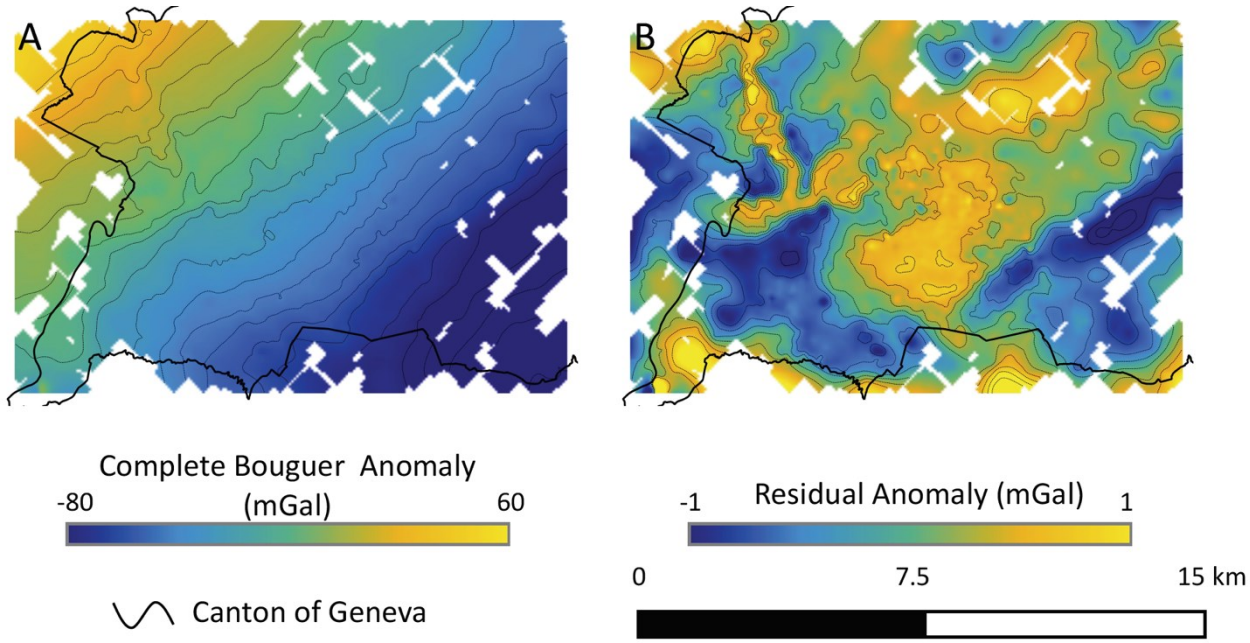

Figure 9 – A: Complete Bouguer Anomaly. B: Residual gravity anomalies over the study area resulting after removing the linear regional trend

The radial averaged power spectrum of the residual gravity anomaly shown deeper sources in the 0.13-0.76 wavenumber range, corresponding to 7900-2500m wavelengths respectively (Figure 10).

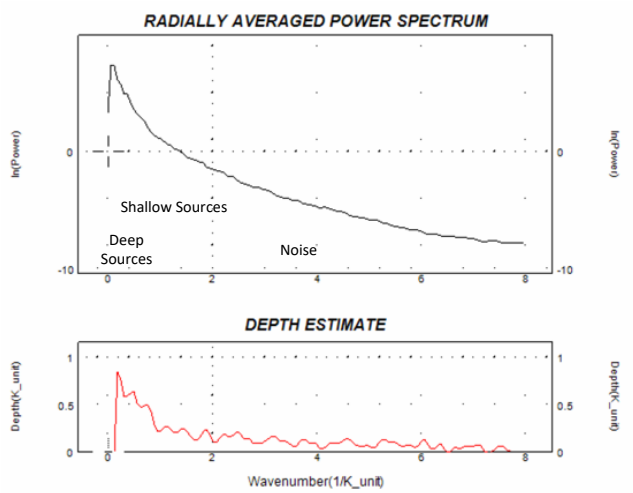

Figure 10 – Radially averaged power spectrum of the residual anomaly

The average depth of the sources generating such anomalies are located at 700m in depth. Shallower sources at 250m in depth as average, are in the 0.44-3 wavenumber range corresponding to the 420- to the 300-2200m wavelength bandwidth (Table 3).

Table 3 – Radially averaged power spectrum bandwidths for the residual gravity anomaly

Wavenumber (1/k_units)	Wavelength (m)	Source average depth (m)
0.13	7900	700
0.76	2500	
0.44	2200	250
3	300	

5. 3D GRAVITY INVERSION PROCESSING

The inversion processing allows to reconstruct the density distribution in the subsurface according to gravity data observed on the field. The GM-SYS 3D toolset in Geosoft Oasis Montaj was used in this task. The inversion processing can provide accurate results when geometrical constraints (i.e. from a 3D geological model) and/or density data for the lithology of interest are available, therefore reducing the uncertainty of the resulting density model.

According to the power spectrum, the base of the Upper Jurassic was set at the lower boundary of the model. Therefore, 4 units were modelled by 3D inversion: Quaternary deposits, Oligecene Molasse sediments and Lower Cretaceous and the Upper Jurassic. Figure 11 shows the 3D gravity response of the 3D model, the residual gravity anomaly and the relative misfit.

Initially the density variations limits was set according to the data available (Table 2). The results of the inversion are shown in Figure 12. It is possible to observe how the misfit was only slightly reduced. The geologic units below Upper Jurassic were tested in terms of inversion, but the final results didn't show any significant difference.

Therefore we removed the density variations constrain and the results are shown in Figure 13, where it is possible to highlight how the misfit between the gravity field observations and the gravity response of the model.

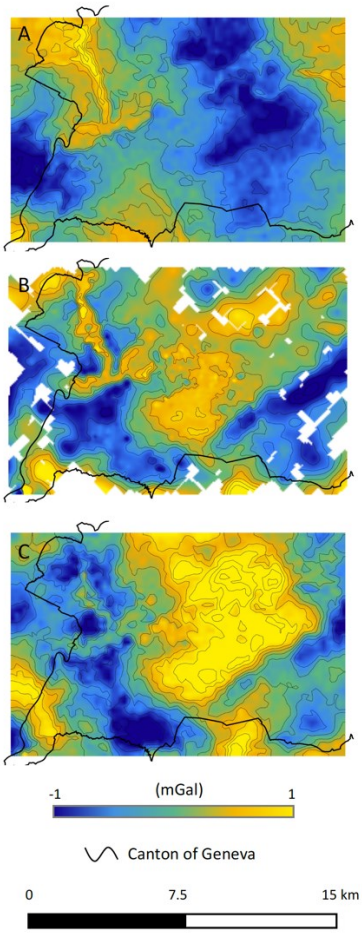

Figure 11 – A: Gravity effect of the 3D geological model; B: Residual gravity anomaly from field observations; C: Misfit

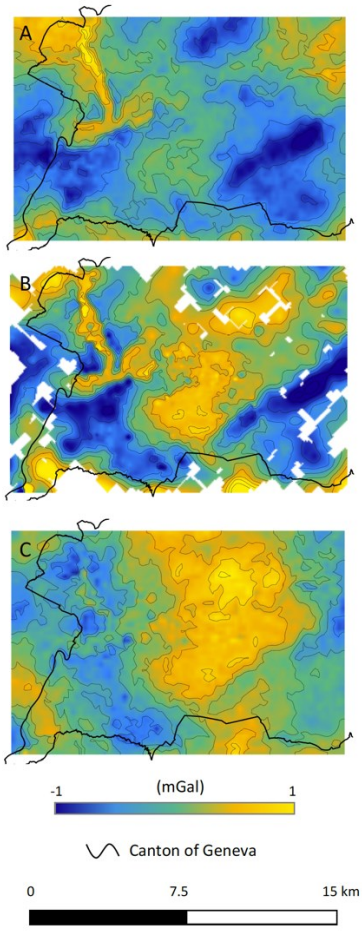

Figure 12 – A: Gravity effect of the 3D geological model after density constrained inversion modelling; B: Residual gravity anomaly from field observations; C: Misfit

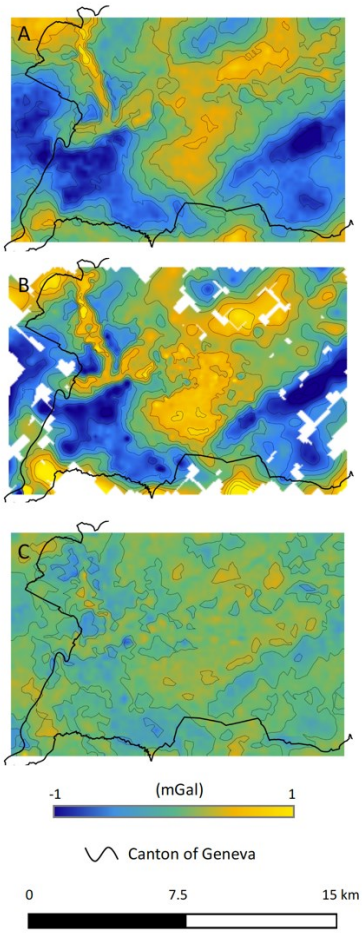

Figure 13 – A: Gravity effect of the 3D geological model after inversion modelling; B: Residual gravity anomaly from field observations; C: Misfit

Table 3 and Figure 14 show the results of this final step of inversion processing.

Table 3 – Density values after 3D Inversion for the target geologic formations

Formation	Min	Max	Average	SD
Quaternary	2.33	2.36	2.34	0.004
Oligecene Molasse	2.46	2.6	2.58	0.021
Lower Cretaceous	2.68	2.75	2.71	0.007
Upper Jurassic	2.63	2.75	2.70	0.015

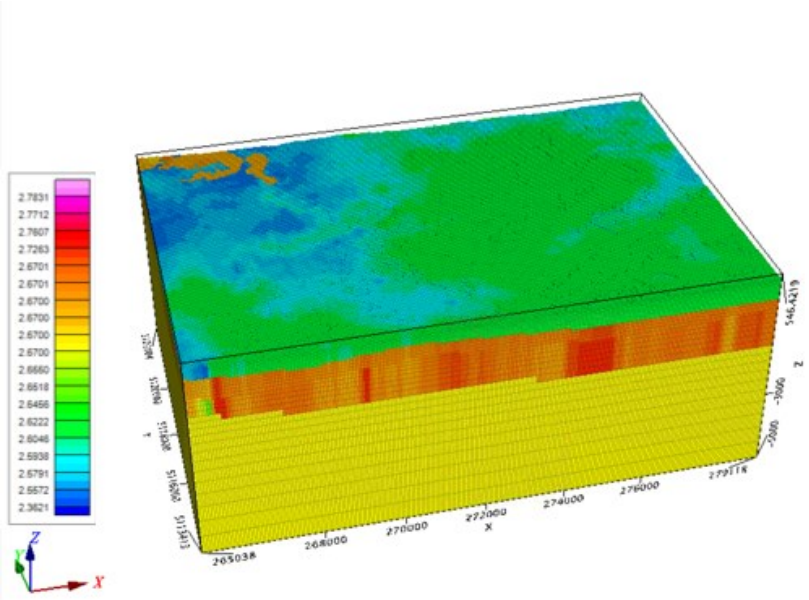

Figure 14 – 3D density model resulting after inversion processing

6. CONCLUSION

The gravity survey carried out in the Geneva area shows the potential of the gravity method in constraining a realistic density model distribution model of the subsurface.

Quaternary deposits, Oligocene Molassic sediments and Upper Mesozoic units were constrained by 3D inversion modelling starting from the residual gravity anomaly produced after collecting new gravity data in the study area.

However, the gravity method itself, shows some limitations in particular in defining vertical density variations and the results of the 3D inversion show encouraging results which can only be improved by the integration with other geophysical data such as S-waves active seismic to better constrain the geometry of the Quaternary deposits and 3D Distributed Acoustic Sensing Vertical Seismic Profiling which will be collected in summer 2019 to complete the set of data required for an accurate subsurface uncertainty assessment over the study area.

AKNOWLEDGEMENTS

The present study is part of GECOS (Geothermal Exploration Chance Of Success), a project (no. 26728.1 PFIW-IW) co-funded by INNOSUISSE and by Services Industriels de Genève and GEO2X SA.

This paper is also a contribution to the national Swiss research program SCCER SoE.

7. REFERENCES

Abdelfettah, Y., Schill, E., & Kuhn, P. (2014). Characterization of geothermally relevant structures at the top of crystalline basement in Switzerland by filters and gravity forward modelling. *Geophysical Journal International*, *199*(1), 226–241. https://doi.org/10.1093/gji/ggu255

Affolter, T., & Gratier, J.-P. (2004). Map view retrodeformation of an arcuate fold-and-thrust belt: The Jura case. *Journal of Geophysical Research*, *109*(B3). https://doi.org/10.1029/2002jb002270

Allis, R. G., Gettings, P., & Chapman, D. S. (2000). Precise gravimetry and geothermal reservoir management. *Twenty-Fifth Workshop on Geothermal Reservoir Engineering*, (February 2002), 1–10.

Altwegg, P. (2015). *Gravimetry for Geothermal Exploration*. University of Neuchatel.

Angelillo, V. (1983). Les Marnes et Grès gris à gypse («Molasse grise») du bassin genevois. In Université de Geneve (Ed.), *Géologie, sédimentologie, stratigraphie.* Geneva.

Arn, R., Conrad, M. A., & Weidmann, M. (2005). *Nyon. Atlas géologique de la Suisse 1:25'000, feuille N° 117 and explanatory note*. Bern.

Becker, A. (2000). The Jura Mountains — an active foreland fold-and-thrust belt? *Tectonophysics*, *321*, 381–406.

Blakely, R. J. (1995). Potential theory in gravity and magnetic applications. In *Journal of Applied Geophysics* (Vol. 36). https://doi.org/10.1016/s0926-9851(96)00039-0

Brentini, M. (2018). *Impact d'une donnée géologique hétérogène dans la gestion des géo-ressources: analyse intégrée et valorisation de la stratigraphie à travers le bassin genevois (Suisse, France).* Terre & Environnement 140.

Carrier, A., Lupi, M., Clerc, N., Rusillon, E., & Do Couto, D. (2017). Inferring lateral density variations in Great Geneva Basin, western Switzerland from wells and gravity data. *Geophysical Research Abstracts Vol. 19*.

Charollais, J., Weidmann, M., Berger, J. P., Engesser, B., Hotellier, J. F., Gorin, G., … Schäfer, P. (2007). La Molasse du bassin franco-genevois et son substratum. *Archives Des Sciences*, *60*(2–3), 59–174.

Charollais, J., Wernli, R., Mastrangelo, B., Metzger, J., Granier, B., Martin, M. Saint, & Weidmann, M. (2013). Présentation d'une nouvelle carte géologique du Vuache et du Mont de Musièges. *Archives Des Sciences*, *66*, 1–63.

Clerc, N., Rusillon, E., Moscariello, A., Renard, P., Paolacci, S., & Meyer, M. (2015). Detailed Structural and Reservoir Rock Typing Characterisation of the Greater Geneva Basin, Switzerland, for Geothermal Resource Assessment. *World Geothermal Congress 2015, Melbourne, Australia*, (April), 11. https://doi.org/10.1002/2017EF000724

Doyen, P. (2007). *Seismic Reservoir Characterization: An Earth Modelling Perspective*. https://doi.org/10.3997/9789073781771

Gorin, G., Signer, C., & Amberger, G. (1993). Structural configuration of the western Swiss Molasse Basin as defined by reflection seismic data. *Eclogae Geologicae Helvetiae*, *86*(3), 693–716.

Guellec, S., Mugnier, J.-L., Tardy, M., & Roure, F. (1990). Neogene evolution of the western Alpine foreland in the light of ECORS data and balanced cross-section. *Deep Structure of the Alps*, *156*, 165–184. Retrieved from http://cat.inist.fr/?aModele=afficheN&cpsidt=4341857

Guglielmetti, L., Poletto, F., Corubolo, P., Bitri, A., Dezayes, C., Farina, B.M., Martin, F., Meneghini, F., Moscariello, A., Nawratil de Bono, C., Schleifer, A. (2020). Results of a walk-above VSP survey acquired at the Thônex-01 Geothermal well (Switzerland) to delineate fractured carbonate formations for geothermal development. Geophysical Prospecting. In Press

Guglielmetti, L., Comina, C., Abdelfettah, Y., Schill, E., & Mandrone, G. (2013). Integration of 3D geological modeling and gravity surveys for geothermal prospection in an Alpine region. *Tectonophysics*, *608*, 1025–1036. https://doi.org/10.1016/j.tecto.2013.07.012

Homberg, C., Bergerat, F., Philippe, Y., Lacombe, O., & Angelier, J. (2002). Structural inheritance and cenozoic stress fields in the Jura fold-and-thrust belt (France). *Tectonophysics*, *357*(1–4), 137–158. https://doi.org/10.1016/S0040-1951(02)00366-9

Kahle, H. G., Klingele, E., Mueller, S., & Egloff, R. (1976). The variation of crustal thickness across the Swiss Alps based on gravity and explosion seismic data. *Pure and Applied Geophysics PAGEOPH*, *114*(3), 479–494. https://doi.org/10.1007/BF00876947

Kempf, O., & Pfiffner, O. A. (2004). Early Tertiary evolution of the North Alpine Foreland Basin of the Swiss Alps and adjoining areas. *Basin Research*, *16*(4), 549–567. https://doi.org/10.1111/j.1365-2117.2004.00246.x

Klingele, E. (2006). Systematic analysis of the Bouguer anomalies of Switzerland. *Jahresberichte 2006, Schweizerische Geophysikalische Kommission SGPK*, 13.

Kuhlemann, J., & Kempf, O. (2002). Post-Eocene evolution of the North Alpine Foreland Basin and its response to Alpine tectonics. *Sedimentary Geology*, *152*(1–2), 45–78. https://doi.org/10.1016/S0037-0738(01)00285-8

Mauri, G., Marguet, L., Jansen, G., Marti, U., Baumberger, R., Allenbach, R., … Miller, S. A. (2017). COMBINED USE OF LAND GRAVITY DATA AND 3D GEOLOGICAL MODEL TO IMAGE DEEP GEOLOGICAL BASIN : CASE OF REGION of la Broye, Switzerland. *Proceedings of 46th IASTEM International Conference*, (February). Seoul.

Mazurek, M., Hurford, A. J., & Leu, W. (2006). Unravelling the multi-stage burial history of the Swiss Molasse Basin: Integration of apatite fission track, vitrinite reflectance and biomarker isomerisation analysis. *Basin Research*, *18*(1), 27–50. https://doi.org/10.1111/j.1365-2117.2006.00286.x

Meyer, M. (2000). *Le Complexe récifal kimméridgien-tithonien du Jura méridional interne (France), évolution multifactorielle, stratigraphique et tectonique*. Thèse de doctorat: Univ. Genève, 2000 - Sc. 3170 – 2000.

Montadon, L. (2000). *Etude gravimétrique de la région du LEP (CERN, Genève). Modélisation tridimensionnelle du sous-sol et détermination des variations de densités du Quaternaire àl'aide du gradient gravifique vertical mesuré*.

Moscariello, A. (2016). Geothermal exploration in SW Switzerland. *European Geothermal Congress 2016, Strasbourg, France*, 9.

Moscariello, A. (2019). The geomorphological landscapes in the Geneva Basin. In E. Reinard (Ed.), *Landscapes and landforms of Switzerland* (p. 15). Springer Verlag.

Moscariello, A., Gorin, G., Charollais, J., & Rusillon, E. (2014). Geology of Western Switzerland and nearby France in a Geo-Energy perspective. *19th International Sedimentological Congress*, (August), 25.

Moscariello, A., Guglielmetti, L., Omodeo-Salé, S., De Haller, A., Eruteya, O.-E., Lo, H.-Y., … Meyer, M. (2020). Heat production and storage in Western Switzerland: advances and challenges of intense multidisciplinary geothermal exploration activities, 8 years down the road. *World Geothermal Congress 2020*, submitted for publication. Reykjavik, Iceland.

Nettleton, L. L. (1939). Determination of Density for Reduction of Gravimeter Observations*. *Geophysics*, *4*(3), 176–183. https://doi.org/10.1190/1.0403176

Olivier, R., Dumont, B., & Klingelé, E. (2002). L'Atlas gravimetrique de la Suisse. *Schweizerische Geophysikalische Kommission*, (43).

Paolacci, S. (2012). *Seismic facies and structural configuration of the Western Alpine Basin and its substratum (France and Switzerland)*. Geneva.

Parasnis, D. S. (1951). A study of rock density in the English Midlands. *Mon. Not. R. Astron. Soc. Geophys. Suppl.*, *6*, 252–271.

Poldini, E., Burri, J. P., & Inagaki, M. (1963). Les anomalies gravifiques du canton de Genève. *Matériaux Pour La Géologie de La Suisse.,*.

Reynolds, J. M. (1996). *An Introduction to Applied and Environmental Geophysics, 2nd Edition*.

Rusillon, E. (2018). *Characterisation and Rock Typing of Deep Geothermal Reservoirs in the Greater Geneva Basin*. Terre & Environnement 141.

Signer, C., & Gorin, G. (1995). New geological observations between the Jura and the Alps in the Geneva area, as derived from reflection seismic data. *Eclogae Geol. Helv.*, *88/2*, 235–265.

Sommaruga, A. (1999). Décollement tectonics in the Jura foreland fold-and-thrust belt. *Marine and Petroleum Geology*, *16*(2), 111–134. https://doi.org/10.1016/S0264-8172(98)00068-3

Telford, W. M., Geldart, L. P., & Scheriff, R. E. (1990). *Applied Geophysics* (Cambridge University Press, Ed.). Cambridge University Press.

Uwiduhaye, J. d. A., Mizunaga, H., & Saibi, H. (2018). Geophysical investigation using gravity data in Kinigi geothermal field, northwest Rwanda. *Journal of African Earth Sciences*, *139*, 184–192. https://doi.org/10.1016/j.jafrearsci.2017.12.016

Wagner, J. J., Gong, G., Fanelli, M., Jordi, S., & Rosset, P. A catalogue of physical properties of rocks from the Swiss Alps and nearby areas. , Atelier d'impression, Université de Genève § (1999).

Wilkinson, M., Mouli-Castillo, J., Morgan, P., & Eid, R. (2017). Time-lapse gravity surveying as a monitoring tool for CO2 storage. *International Journal of Greenhouse Gas Control*, *60*, 93–99. https://doi.org/10.1016/j.ijggc.2017.03.006